Profiles of alkali concentration and galactoglucomannan degradation in kraft impregnation of Scots pine wood. Experimental observations and modeling.

Pablo Nicolás Montagna[1], Kaarlo Nieminen[2], María Cristina Inalbon[1(*)], Herbert Sixta[2], Miguel Angel Zanuttini[1*].

[1]Instituto de Tecnología Celulósica, Facultad de Ingeniería Química, Universidad Nacional del Litoral. Santiago del Estero 2654, Argentina. Tel: +54-342-4520019.

[2]Department of Forest Products Technology, Aalto University, FI-00076 AALTO, Finland. Tel: +358-9-470-28176.

cinalbon@fiq.unl.edu.ar

Abstract:A deep understanding of alkali impregnation including the profiles of alkali concentration and hemicellulose degradation is necessary to analyze the optimization of current and innovative processes. In this paper, the impregnation processof *Pinussylvestris* wood is analyzed and modeled under consideration of deacetylation, reactions of acidic group, and galactoglucomannan (GGM) degradation. The immobile anionic groupsactivated by the ionization of lignin derived OH groups are also considered for the assessment of the Donnan effect. Predicted profiles of sodium and hydroxide ions and acetyl group concentrations are compared to experimental results. The balance between impregnation and hemicellulose degradation levels is discussed based on the developed models. Expectedly, higher concentrations and temperatures speed up the impregnation process. Nevertheless, a higher OH^- concentration has the benefits for the same impregnation front position thatthe alkali charge inside the chip is higher and the GGM degradation is lower.

Keywords: acid group reactions: acetyl group content;deacetylation;Donnan effect; ionic diffusion; model validation; pulping process

Introduction

Background and goals

A deep understanding of alkali impregnation including the profiles of alkali concentration and hemicellulose degradation is necessary to analyze the optimization of current and innovative pulping processes.Incomplete impregnation increases the amount of uncooked rejects and affects pulping yield as well as uniformity, strength and bleachability of the pulp (Gullichsen et al. 1992, Gullichsen et al. 1995, Malkov et al. 2002).The ideal impregnation brings the alkaline reagent in the interior of the wood chip as rapidly as possible.In reality,a high proportion of the diffusing alkali into the chips is consumed by chemical reactions and this has a detrimental effect on the dissolvedhemicellulose fraction. The effects of the impregnation performance on final properties of the obtained pulp is well investigated (Höglundat all. 1994; Gullichsenet al. 1995; Bykovaet al. 1997; Svedmanand Tikka, 1998; Malkovet al. 2001; Ban y Lucia, 2003; Ban et al. 2003).

Chip thickness, which may correspond to radial (R) or tangential (T) wood direction, is the critical dimension for diffusion of cooking chemicals (Gullichsen et al. 1992, Gullichsen et al. 1995). The relation of chip thickness tokraft pulp uniformity wasinvestigated by numerous authors (Borlew and Miller 1970;Akhtaruzzaman and Virkola 1979;Gullichsen et al. 1992;Gullichsen et al. 1995). For quantitative analysis of the impregnation process, a 1D-balance along the transverse direction of the wood is a useful approach.

For a rigorous modeling of aspecific wood, two relationshipsare especially important: a) an expression of the ion permeability of the wood as a function of variables, as permeability affects the effective diffusion of each species and, b) a kinetic expression of the reactions which are involved in the process. The extent of the reactions and the local dynamic effective diffusion coefficients should be known for the resolution of the differential equation system that results

from the mass balance. Moreover,there is a difference between ionconcentrations in the solution outside the chips and the concentrationsionized acid groups in wood. The impact of Donnan effect on kraft cooking impregnation was discussed in detail by Kuitunen et al. (2013). For Eucalyptus wood, a model was derived that includes all these aspects of the kraft impregnation process. The predicted concentration profiles were quite close to those of the experimental results (Inalbon et al. 2009, 2011).

In case of softwoodimpregnation,the deacetylation and the degradation of hemicelluloses play an essential role.Paananen et al. (2010) showed for *Pinussylvestris* under conditions of kraft impregnation (80 – 130ºC and 0.3to 1.55 $molL^{-1}$ $[OH^-]$)that the degradation of galactoglucomannans (GGM)is very relevant. In the quoted study, the peeling-off reaction was considered,in which monomer units are progressively eliminated from the reducing end-groups and subsequently transformed into isosaccharinic acids (ISA). Moreover, the stopping reaction was also modeled that takesplace when the reducing end-group is converted into an alkali-stable metasaccharinic acid (MSA) group.The base-catalyzed cleavage of glycosidic bonds at high temperatureshas also to be accounted forbecause this reaction generates new reducing end-groups, which undergo further peeling reactions.

In the present paper, the impregnation process of *Pinussylvestris* wood is analyzed. Deacetylation and the acid group reactions, together with GGM degradation, will be considered for modeling.At pH higher than 10.5, additional immobile anionic groups are arising due to the gradual ionization of the OH groups of lignin, and these will also be taken into account not only for the calculation of alkali consumption but also for the assessment of the Donnan effect. Predicted profiles of sodium and hydroxide ions and acetyl group concentrations should

becompared with those of the experimental results. The models will be discussed in terms of the balance between impregnation level and hemicellulose degradation.

Departing model

A model for the 1D isothermal alkali impregnation process of eucalyptus chipsis already described (Inalbon et al. 2011). Briefly, Na^+, OH^-, and SH^-ions and acetate groups were considered as mobile ions, and acetyl and acid groups of wood were considered as immobile. Assuming that wood is already saturated in water, the impregnation can be described as a reacting non-convective diffusion process in a pseudo-homogeneous solid. Then, the mass balance equation is:

$$\frac{\partial C_i}{\partial t} + \frac{\partial N_i}{\partial x} = R_i \qquad (1)$$

whereC_i is the concentration of ion *i* ($molL^{-1}$), *t* is the time (min), N_i is the net molar flux of ion *i* [$mol \cdot cmL^{-1} \cdot min^{-1}$], R_i is the chemical consumption or generation rate of ion *i*[$mol\ L^{-1} \cdot min^{-1}$]. Under ideal solution behavior, the net molar flux can be expressed as a function of the ion electrochemical potential:

$$N_i = - \left(D_i^{eff} \cdot \frac{\partial C_i}{\partial x} + \frac{z_i \cdot D_i^{eff} \cdot C_i \cdot F}{R \cdot T} \cdot \frac{\partial \phi}{\partial x} \right) \qquad (2)$$

whereϕ is the electric potential (V), D_i^{eff} is the effective diffusion coefficient (cm^2min^{-1}), *x* is the position in the direction of analysis, $z_i$is the ion valence, *T* is the temperature (K), *R* is the universal gas constant (8.3145 $Jmol^{-1} \cdot K^{-1}$) and *F* the Faraday constant (96487 J/mol·V).
The condition of zero electric current is applied. It considers all species (i=1,…j) and allows writing the electric potential derivative as a function of concentrations and diffusion coefficients:

$$\frac{\partial \phi}{\partial x} = - \frac{R \cdot T}{F} \frac{\sum_{i=1}^{i=j} z_i \cdot D_i^{eff.} \frac{\partial C_i}{\partial x}}{\sum_{i=1}^{i=j} z_i^2 \cdot D_i^{eff} \cdot C_i} \qquad (3)$$

Combining equations(2) and (3), the mass balance in equation (1) becomes:

$$\frac{\partial C_i}{\partial t} = R_i + \frac{\partial}{\partial x} \left(D_i^{eff.} \frac{\partial C_i}{\partial x} - z_i \cdot D_i^{eff} \cdot C_i \cdot \frac{\sum_{i=1}^{i=j} z_i \cdot D_i^{eff.} \frac{\partial C_i}{\partial x}}{\sum_{i=1}^{i=j} z_i^2 \cdot D_i^{eff} \cdot C_i} \right) \qquad (4)$$

The effective ion diffusion in the transverse direction of wood is expressed as the product of the wood effective capillary cross-sectional area (*ECCSA)*(dimensionless) in this direction and the ion diffusion coefficient in solution D_i^0($cm^2 min^{-1}$):

$$D_i^{eff} = D_i^0 \,.\, ECCSA = \frac{R \,.\, T \,.\, \lambda_i^0}{|z_i| \,.\, F^2} ECCSA \qquad (5)$$

where$\lambda^0{}_i$ is the ion mobility ($cm^2/\Omega \cdot eq$).ECCSA is the variable that involves the dynamic wood changes due to the alkali actions.

As the acid groups cannot leave the wood, the solution within the wood tissue is quasi separated from the external solution by a semipermeable membrane, which confines the acid groups but allows transporting water and all simple ions (Grignon and Scallan 1980).At neutral pH, theimmobile anionicgroups in the cell wall are carboxyl groups, butunder alkaline conditions, phenolic hydroxyl groups are additionally ionized.The Donnantheory considers that, at equilibrium,the chemical potential and the activity coefficient of each mobile species are equal on both sides of the interphase (Donnan and Harris 1911). Disregarding any osmotic pressure gradient, a constant ratio λ_D between the concentration inside and outside the wood ($C_i|_I$ and $C_i|_E$, respectively) is obtained:

$$\lambda_D = \frac{C_{OH^-}|_E}{C_{OH^-}|_I} = \frac{C_{SH^-}|_E}{C_{SH^-}|_E} = \frac{C_{Na^+}|_I}{C_{Na^+}|_E} \qquad (6)$$

Equation (6) expresses the fact that for negative mobileions the concentration at the wood side of the interphase is lower than the one in the liquor (λ_D>1). The opposite occurs for positive ions.

A balance involving fixed and mobile charged species has to be satisfied at any place of the wood including wood surface.

$$z_{OH^-}\cdot C_{OH^-}|_I + z_{SH^-}\cdot C_{SH^-}|_I + z_{Acetate}\cdot C_{Acetate}|_I + z_{Na^+}\cdot C_{Na^+}|_I + z_{AG^-}\cdot C_{AG^-}|_I + z_{PhO^-}\cdot C_{PhO^-}|_I = 0 \qquad (7)$$

$$z_{OH^-}\cdot C_{OH^-}|_E + z_{SH^-}\cdot C_{SH^-}|_E + z_{Na^+}\cdot C_{Na^+}|_E = 0 \qquad (8)$$

The Donnan coefficient is obtained after solving equations 6, 7, and 8.

Refined model

In this paper, the model previously derived is adapted to *P.sylvestris* wood. The specific deacetylation kinetics (Montagna et al. 2013) is used andthe model is refined considering: a) The GGM degradationkinetics according to Pannanen et al. (2010), and Montagna et al.(2013), and b) The ionization of phenolic hydroxyl (OH_{phen}) groups oflignin. This ionization produces additional alkali consumption and generates extra immobile anionic groups.

The kinetic expression for the deacetylation was alreadyreported (Montagna et al.2013):

$$R = R_{Acetyls} = -k \cdot \left(C_{acetyls}\right)^n \cdot (C_{NaOH})^m = -A\cdot e^{\left(\frac{-E}{R\cdot T}\right)} \cdot \left(C_{acetyls}\right)^n \cdot (C_{OH})^m \qquad (9)$$

Where (*k)*is the kinetic constant, (*n* and *m*) the reaction order, (*A*) the pre-exponential factors and (*E*) the activation energy. In this model, the hydrolysis of esters or lactones involves reactions of lower significance and thus they are considered to be coupled to the deacetylation degree. This hydrolysis releases additional immobile carboxyl groups.

Galactoglucomannan (GGM) degradation:The kinetic model describing alkaline degradation of carbohydrates proposed by Paananen et al. (2010)is adopted in this work. It was derived for conditions corresponding topulping impregnation and took into accountthe peeling/stopping (first order) reactions, (Scheme 1):

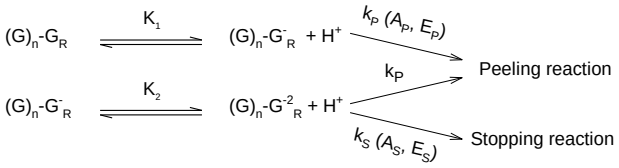

and the base-catalyzed cleavage of glycosidic bonds (simplified), (Scheme 2):

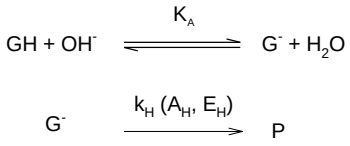

Where:$(G)_n$-G_R, $(G)_n$-G_R^-, $(G)_n$-$G_R^{=}$: GGM with neutral, mono or dianionic reducing end-group.GH, G^- : neutral GGM and GGM after the deprotonation reaction.k_P, k_S, k_H: rate constants for peeling, stopping and alkaline hydrolysis reactions.A_P, A_S, A_H: pre-exponential factors for peeling, stopping and alkaline hydrolysis reactions.E_P, E_S, E_H: activation energies for peeling, stopping and alkaline hydrolysis reactions.K_1, K_2, K_A: ionization equilibrium constants.

Paananen et al. (2010) fitted this model to experimental data (GGM mass fraction) obtained at 80-130ºC and effective alkali ranging 0.31-1.55 mol OH^-L^{-1}. In a later work,an extended range wastaken into account paying attention to milderconditions (Montagna et al. 2013). The temperature range was 50 - 130ºC and the concentration range was 0.1 - 1.55 mol OH^-L^{-1}, and the parameters were obtained by fitting the combined data to the model.

The whole set of differential equations related to Scheme 1 can be solved by assuming the following mass balance:

$$GGM=[G_{IS}]-[G_E]-[P] \quad (10)$$

Where: G_{IS}: is the carbohydrate mole fraction insoluble in alkali, G_E: is the mole fraction of eliminated end-groups, andP is the degradation product.

The dependence of ECCSA on temperature, time, and hydroxide concentration is complex and difficult to express mathematically. Nevertheless, ECCSA can be better related to the degrees of reaction. Montagna et al. (2013) found the following expression of ECCSA as a function of acetyl (AcG), GGM contents and temperature for pine wood:

$$ECCSA=0.573+\left[0.224\cdot AcG-0.0013\cdot AcG\cdot T+0.0002\cdot AcG^2\cdot T\right]$$
$$+\left[-0.867\cdot GGM^2-0.0018\cdot GGM\cdot T+0.0033\cdot GGM^2\cdot T\right] \quad (11)$$
$$R^2_{adjusted}= 98.0\ \%.$$

The expression indicates that, when wood is alkali treated, the ECCSA-value, which measures ion permeability, does not depend on alkali concentration. Instead, it depends on the degree of the reactions that the alkali produces (Inalbon et al. 2013). It was shown that theECCSA-value is not reduced when alkali is removed by washing. As discussed in previous studies, for eucalyptus wood, it depends on the deacetylation degree (Inalbon and Zanuttini 2008) and, for pine wood, it depends on both thedeacetylation and GGM degradation degree (Montagna et al. 2013).

Initial conditions and concentrations are summarized in Table 1.The initial concentrations of $HS^{-1}$and OAc^{-1} ions in wood are zero. The initial concentrations of OH^- and H^+ in wood are given by the water constant equilibrium. The initial value of acetyl group, acid group and unreacted acid group contents in wood ($C_{Ac;}\ C_{AG;}\ C_{UAG}$respectively) correspond to those in the untreated wood. The initial sodium content (C_{Na}) is equal to the original free acid group content.The initial concentrations for GGM, G_E, G_R and Pare adopted from Paananen et al. (2010).

Boundary conditions need to be specified for mobile ions, such as OH^-, SH^-, Na^+, and CH_3COO^- ions. The species flux at the chip center ($x=h/2$) is zero; h is the chip thickness.

$$N_{i(x=h/2;\forall t)} = 0 \quad (12)$$

External mass transfer restrictions are neglected. At the liquor-wood (L/W) interphase ($x=0$), a pseudo equilibrium is considered. According to theDonnan equilibrium, concentration at the wood side of the interphase ($C_{OH|I}$) can be obtained from the corresponding concentration in the liquor ($C_{OH|E}$) fromequation (6).The Donnan coefficient is calculated by theequations6, 7, and 8.

Numerical resolution

In order to solve the differential equation system resulting from Eq. 1 (there are "i" equations, one for each species) a finite difference method was used. The application of this method transforms derivatives into finite differences that approximate them. In a second step, a resolution algorithm is applied.First, the spatial domain (half chip thickness) was discretized dividing it into N_x identical segments (generating N_x+1 nodes) (Figure 1), and the time domain (impregnation time), was divided into N_{time} periods.Then, forward differences were used to approximate the time derivative and centered ones for the spatial derivative.The resulting system is:

$$(C_i)_k^{t+1} = (C_i)_k^t - \Delta t \cdot \frac{(N_i)_{k+\frac{1}{2}}^t - (N_i)_{k-\frac{1}{2}}^t}{\Delta x} + \Delta t \cdot (R_i)_k^t \qquad (13)$$

where:

$$\Delta x = \frac{\text{Half chip tickness}}{Nx} \quad \text{and} \quad \Delta t = \frac{\text{Impregnation time}}{Ntime}$$

The subscript *i*indicates the species, and *k* and *t* are the space and time nodes. This equation is solved at every pair k,t for each species i, all over the time and space domains, i.e., from t=1 to

t=Ntime+1 and from k=1 to k=Nx+1. The molar flux derivative is approximated considering the fluxes at the *k+1/2* and *k-1/2* positions. Eq.14 gives the flux at *k+1/2*:

$$(N_i)^t_{k+\frac{1}{2}} = -(D_i)^t_{k+\frac{1}{2}} \cdot \frac{(C_i)^t_{k+1} - (C_i)^t_k}{\Delta x} + z_i \cdot (D_i)^t_{k+\frac{1}{2}} \cdot (C_i)^t_k \cdot \frac{\sum_{i=1}^{i=i} z_i \cdot (D_i)^t_{k+\frac{1}{2}} \cdot \frac{(C_i)^t_{k+1} - (C_i)^t_k}{\Delta x}}{\sum_{i=1}^{i=i} z_i^2 \cdot (D_i)^t_{k+\frac{1}{2}} \cdot (C_i)^t_k} \qquad (14)$$

Concentration derivatives in (14) are approximated by forward differencesfor the *k+1/2* node (forward with respect to node *k*) but backward differences are used for the *k-1/2* node (not shown). The diffusion coefficient results from the average between the *k+1/2* and *k-1/2* positions:

$$(D_i)^t_{k+\frac{1}{2}} = (ECCSA)^t_{k+\frac{1}{2}} \cdot D_i^\circ = \frac{1}{2}\left[(ECCSA)^t_{k+1} + (ECCSA)^t_k\right] \qquad (15)$$

Finally, theboundary conditions were also discretized.

Computational aspects

The numerical resolution of the discretized differential equation system was performed using Matlab®. The resulting Matlab script can be summarized as follows. Parameter specification:All parameters that will be used later in the algorithm are defined: Temperature, effective alkali, sulphidity, activation energies, diffusion coefficients, etc.Initial conditions: The initial value for each of them is specified, according to the initial conditions.Time loop: Inside this loop, calculations are performed at every time step, from t=1 to t=ntime.

Boundary condition #1*:*As the boundary condition is time-dependant, species concentrations at k=1 are calculated (together with the Donnan coefficient) at the beginning of this time loop.

Auxiliary calculations*:* Variables determined in this part are: $ECCSA]^t_{k+\frac{1}{2}}$, $ECCSA]^t_{k-\frac{1}{2}}$,$D_i]^t_{k+\frac{1}{2}}$, $D_i]^t_{k-\frac{1}{2}}$, $N_i]^t_{k+\frac{1}{2}}$,$N_i]^t_{k-\frac{1}{2}}$, and $R_i]^t_k$.Space loop: For each time t, $C_i]^{t+1}_k$is calculated for each species,

from k=2 to k=Nx.Boundary condition #2: $C_i]^t_{Nx+1}$ for each species is calculated (symmetric concentration profile).

Materials and methods

Air dried *P. sylvestris* wood blocks with sides of 35 mm were prepared. In a closed reactor, wood blocks were steamed and then drawn down in the thermostated impregnation liquor. The L/W ratiowas high enough (aprox. 1000 Lkg^{-1}) to ensure constant chemicals concentration in the external liquor during impregnation. Afterwards, the system pressure was increased to 0.6 MPa. Blocks were kept under pressure and agitation. Once the treatment time was reached, the reactor was depressurized, and the blocks were taken off and immediately immersed into liquid nitrogen. Then, they were stored in a freezer at -10ºC. The experimental conditions are shown in Table 2; the sulfidity was 30% for each case.

The frozen blocks were sliced with a carpentry saw to remove the layers of impregnated wood, except for the block faces of interest (tangential faces). These faces were then cut into 200 μm-thick serial slices. Slices were weighed, and their alkali and sulfide contents were determined by the quantitative neutralization of 20 mL of water containing the slice (SCAN-N2:63). The sodium concentration in the liquid volume resulting from titration was determined by AAS. The wood OAcgroup content was estimated by diffuse FTIR, directly applied on the dry slices. Theratio between the band intensity at 1735 cm^{-1}(normalized to the 1510 cm^{-1} band) and the OAc content determined by GC were the basis of the calculations (Zanuttini et al. 1998).

Results and discussion

General pattern indicated by the experimental results

Figure 2.a shows the experimental profiles obtained for pine wood treated with 0.45 $molL^{-1}$NaOH, 28.9% sulfidityat 105°C for 30 min. The general patterns that were previously found for hardwood looks similarto those of pine.The profile of acetyl groups looks like a sigmoid-shaped profile moving toward the chip center and the alkali concentration gradually decreases from the interphase to zero in the impregnation front. In terms of the unreacted core model, the reactive processes are faster than the alkali diffusion process.

The Na^{+}concentration, which must be equivalent to the total of the concentrations of the negative ions, is always clearly higher than the hydroxyl ion concentration. The figure also shows that the hydrosulfide and alkali impregnations are simultaneous.There is also a drop in the OH^{-} concentration at the interphase, related toexternal liquor concentration (0.45 $molL^{-1}$) due to theDonnaneffect. The lower concentration reduces the driving force for the diffusion, and thus implies a restriction foralkali impregnation.

Model validation

Figure 2.bshows experimental and predicted Na^{+}, H^{S}-, and OH^{-} concentration profiles for the following set of conditions: effective alkali: 0.486 molNaOHL^{-1}; sulfidity: 28.6% S; temperature: 130°C; impregnation time: 20 min.Due to geometric symmetry, the simulation results are plotted for half the chip thickness, i.e., from the woodliquid interphase ($x = 0$) to the chip center ($x = h/2$). Species concentrations in the external liquor, which were kept essentially constant by setting highL/W ratio, are also indicated. Parameters of simulation were Nx = 50; space step: 0.01 cm; time step: 0.01 min.The simulation took 8.7 s calculating with an Intel Core 2 Duo T5600 (@1.83 GHz) CPU with 2 GB RAM.

The model predictions are satisfactory. The transition zone ranging from 1.8 to 2.4 mm is highlighted by dashed vertical lines. In the inner zone, there is no alkali present, and the acetyl content is maintained at the level of the untreated wood (0.5 N). In the outer zone, there are no acetyl groups. The transition zone is a moving impregnation front, whose position at different times allows determining the pace of impregnation.

The impregnation front position is accurately predicted, even though the simulation seems to be ahead of the experimental one. This can be especially noticed in the acetyls profile. The shape of the OH^- profile is not properly followed by the model. The experimental values in the zone close to the chip border have a considerable error because the CO_2 present in air neutralizes the alkali during the laboratory determinations.

Another way to analyze the validity of the model is by comparing experimental and simulated position of the impregnation front. Front position is considered as the distance from the interphase up to theposition where the OH^- concentration is zero; another possible criterion could be the distance from the interphase at which theacetyl content is half that of the initial. Figure 3 shows the simulated impregnation front positions plotted against the experimental results. The accuracy is acceptable at low impregnation times and temperature but, at higher temperature, the similarity is lower.

Analysis of the observations

The model is suitable for simulatingthe profile evolution of species concentrationsas well asthe degree of reaction and kinetics.The deacetylation rate can be calculated and plotted together with acetyl profiles. Figure 4.a shows how the maximum speed rate coincides with the inflection point of the acetyl profile. The shape of the peak is not perfect due to the space step used in the

simulation. A better simulation could be obtained using a smaller space step which implies an increment in the required calculation time. With longer impregnation times, the maximum speed is lower because the alkali concentration near the front is reduced as the front position goes into wood.

Figure 4.b shows simulated GGM profiles at different times for an impregnation with EA: 0.486 molNaOHL^{-1}, S: 28.6%, at 130°C.At the interphase, the GGM weight fraction is quite similartothevalues that can becalculatedby the kinetic expressionofPaananen et al. (2010),which was derived for milled wood, namely 0.82, 0.73, and 0.66 for 10, 20 and 30 min,respectively.This simulation is useful because the experimental determination of the profile of GGM degradation is difficult. The low mass of the slice is not enough for the usual carbohydrate content determination by hydrolysis and chromatographic analysis.

The effect of temperature and alkali concentration on the degree of impregnation can also be analyzed by means of the model. Figure 5.a shows the effects ofhigher temperature and concentration ata 10 min impregnation level. It can be observed (110°C impregnation) that an increase in the liquor concentration from 0.5M to 0.75M produces the advance in theOH^- front position from 0.19 to 0.21cm. The same advance is reached when thetemperature is elevated from 110ºC to 130ºC in an impregnation with 0.5M. Although the front position is the same (0.21cm), the amount of accumulated alkali in the chip is higher for the impregnation with 0.75M at 110ºC. On the other hand, theGGM degradation markedly increases when the temperature is elevated from 110°C to 130°C at the same concentration level.Both, the higher alkali content and thelower GGM degradation indicate that the increase in alkaline liquor concentration is more convenient than the increase in temperature.The same can be observed for a 30-min impregnation in Figure 5.b.As demonstrated by Young et al. (1972) and Paananen et al.

(2010), the stopping rate increases more than the peeling rate with rising OH^- ion concentration at a given temperature. In this way, the increase in GGM degradation progressively slowed down with increasing OH^- ion concentration until at a certain threshold OH^- ion concentration is reached. This explains what is seen in Fig 5 that at a certain penetration depth the GGM content is higher for the combination low temperature - high alkali concentration (e.g. 110°C, 0.75 M [OH^-]) than for the combination high temperature - low alkali concentration (130°C, 0.5 M [OH^-]).

Conclusions

The general impregnation patterns of hardwood (previous results) and pine wood are similar. The model acceptably predicts the difference that is experimentally found between the liquor concentration and the wood liquid interphase concentration due to the Donnan effect. For the conditions analyzed here, the model clearly shows that the hydrosulfide and alkali impregnation is, generally, simultaneous.The effect of the main process variables (external alkali concentration,sulfidity, temperature, time, and chip thickness) can be analyzed through the proposed model. Profiles of alkali, hydrosulfide and sodium concentration as well as the profile of the detrimental GGM degradation can be predicted. The general patterns found for the simulation of the alkali impregnation are in a fair agreement with theexperimental results. In the range of process variables investigated here, an increase in the concentration and temperature speeds up the impregnation process. Nevertheless, a higher concentration produces two benefits for the same impregnation front position: first, a higher alkali charge inside the chip and, second, a lower GGM degradation.It can be expected that these advantages would have a positive effect on the subsequent pulping process.

Acknowledgement: The authors wish to thank UNL (Projects: CAID+D 11-2013 nº: 50020110100059 y CAID+D nº50120110100538), and Consejo Nacional de InvestigacionesCientíficas y Tecnicas (CONICET) (project PIP 114 20110100400) of Argentina for their financial support.The research leading to these results was performed as part of the "Value through Intensive and Efficient Fibre Supply" (EffFibre) research programme of the Finnish Bioeconomy Cluster (FIBIC - former Forestcluster Ltd), Finland. The authors also wish to thank MetsäFibreOy and Tekes – the Finnish Funding Agency for Technology and Innovation - for their financial support.

References

Akhtaruzzaman, A. F.; Virkola, N. E. (1979) Influence of chip dimensions in Kraft pulping.Pap.Puu. 61 (10), 578–580.

Ban, W. and Lucia, L. A. (2003). Enhancing Kraft Pulping Through Unconventional, Higher Sulfide-Containing pretreatment Liquors - A review. Tappi J., 2(3):1-16.

Ban, W., Singh, J., Wang, S., Lucia, L. A. (2003).Kraft Green Liquor Pretreatment of Softwood Chips. Part II: Chemical Effect on Pulp Carbohydrates. J. Pulp Paper Sci., 29(4):114-119.

Bykova, T.; Klevinska, V.; Treimanis, A. (1997). Effect of green liquor pretreatment on pine wood componentes behavior during kraft pulping.Holzforschung 51(5):439-444.

Borlew, P.; Miller, R. (1970) Chip thickness: A critical dimension in Kraft pulping. Tappi 53 (11), 2107–2111.

Donnan, F. G.; Harris, A. B. (1911) The osmotic pressure and conductivity of aqueous solutions of congo-red, and reversible membrane equilibria. J. Chem. Soc.99, 1554.

Grignon, J.; Scallan, A. M. (1980) Effects of pH and neutral salt upon the swelling of cellulose gels. J. Appl. Polym. Sci. 25, 2829–2843.

Gullichsen, J.; Kolehmainen, H.; Sundqvist, H. (1992) On the nonuniformity of the kraft cook. Pap.Puu.74 (6), 486-490.

Gullichsen, J.; Hyvärinen, R.; Sundqvist, H. (1995) On the nonuniformity of the kraft cook. Part 2.Pap.Puu.77 (5), 331.

Höglund, O.; Pehu-Lehtonen, K.; Hjort, A. (1994).Kraft pulping with black liquor pretreatment.
TAPPI Proccedings, Pulping Conference, 1225-1236.

Inalbon, M. C.; Zanuttini, M. (2008) Dynamics of the Effective Capillary cross-sectional area during the alkaline impregnation of eucalyptus wood.Holzforschung62(4):397-401.

Inalbon, M. C.; Mussati, M. C.; Zanuttini, M. A. (2009) Experimental and theoretical analysis of the alkali impregnation of eucalyptus wood.Ind. Eng. Chem. Res.48 (10), 4791-4795.

Inalbon, M. C.; Mussati, M. C.; Mocchiutti, P.; Zanuttini, M. A. (2011) Modeling of alkali impregnation of eucalyptus wood. Ind. Eng. Chem. Res. 50 (5), 2898-2904.

Inalbon, M. C., Montagna, P. N., Galvan, M. V., Demonte, L. M., Zanuttini, M. A. (2013) Wood capillarity and deacetylation during eucalyptus alkaline impregnation. Suphidity effects and comparison between transverse directions.Holzforschung 67(1):41–46.

Kuitunen ,S.; Vuorinen, T.; Alopaeus V. (2013)The role of Donnan effect in kraft cooking liquor impregnation and hot water extraction of wood. Holzforschung 67(5):511–521.

Malkov, S.; Tikka, P.; Gullichsen, J. (2001).Towards complete impregnation of wood chips with aqueous solutions.Part 2.Studies on water penetration into softwood chips.PaperijaPuu, 83(6):468-473.

Malkov, S.; Tikka, P.; Gullichsen, J. (2002) Towards complete impregnation of wood chips with aqueous solutions. Part 4. Effects of front-end modifications in displacement batch kraft pulping. Pap.Puu.84(8):526-530.

Montagna, P. N.; Inalbon M. C.; Paananen M.; Sixta H.; Zanuttini M. A. (2013) Diffusion Dynamics in Pinussylvestris Kraft Impregnation: Effect of Deacetylation and Galactoglucomannan Degradation. Ind. Eng. Chem. Res. 52:3658−3662.

Montagna, P. N. (2013) Kinetics and effective capillarity and inKraft impregnation of*Pinussylvestris*. Master Thesis FIQ- UNL. (in Spanish)

Svedman and Tikka (1998).The use of green liquor and its derivatives in improving kraft pulping.Tappi J. 81(10):151-158.

Paananen, M.; Tamminen, T.; Nieminen, K.; Sixta, H. (2010) Galactoglucomannan stabilization during the initial kraft cooking of Scots pine.Holzforschung64(6):683-692.
SCAN standard method N2:63 (1963). Total, active and effective alkali in white and green liquors.
Young, R.A., Sarkanen, K.V., Johnson, P. G. Allan, G. G.(1972) Marine plant polymers. III. Kinetic analysis of the alkaline degradation of polysaccharides with specific reference to (1,3)-β –D-glucans. Carbohyd. Res. 21:111-122.
Zanuttini, M.; Citroni, M.; Martinez, M. J. (1998) Application of Diffuse Reflectance Infrared Fourier transform spectroscopy to the Quantitative Determination of Acetyl Groups in Wood.Holzforschung 52:263–267.

Table 1: Initial concentrations

Species	Initial conc. (mol L^{-1})	Species	Initial conc. (mol L^{-1})
$C_{OH-}\|_{(t=0,\forall x)}$	10^{-7}	$C_{AG}\|_{(t=0,\forall x)}$	0.044
$C_{H+}\|_{(t=0,\forall x)}$	10^{-7}	$C_{UAG}\|_{(t=0,\forall x)}$	0.056
$C_{acetate}\|_{(t=0,\forall x)}$	0	$C_{GE}\|_{(t=0,\forall x)}$	0
$C_{SH-}\|_{(t=0,\forall x)}$	0	$C_{Pdeg}\|_{(t=0,\forall x)}$	0
$C_{AcG}\|_{(t=0,\forall x)}$	0.21	$C_{GGM}\|_{(t=0,\forall x)}$	0.96 wt.frac.
$C_{Na+}\|_{(t=0,\forall x)}$	0.044	$C_{GR}\|_{(t=0,\forall x)}$	0.0075 wt.frac.

Table 2. Experimental conditions for impregnation of wood blocks

EA* (g NaOH L^{-1})	Temp. (^{O}C)	Time (min)
0.5	105	15-30
0.5	130	10-20-30
1.55	105	30
1.55	130	10

Effective alkali. $EA = C^{E}_{NaOH} + C^{E}_{Na_2S}$

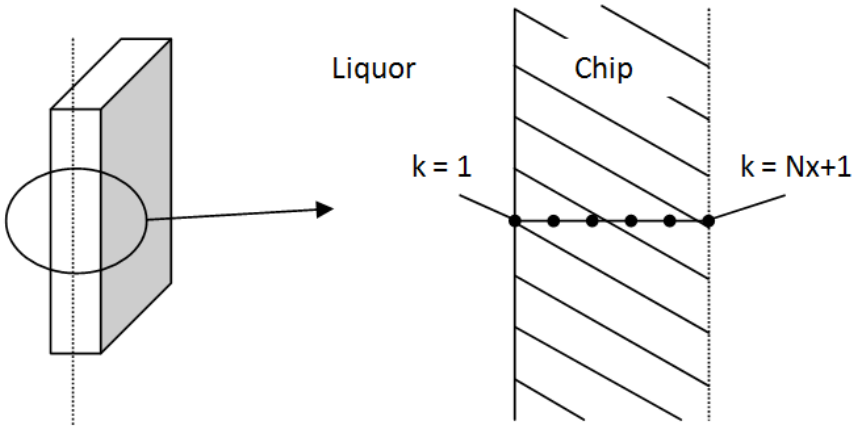

Figure 1. Half chip thickness discretization.

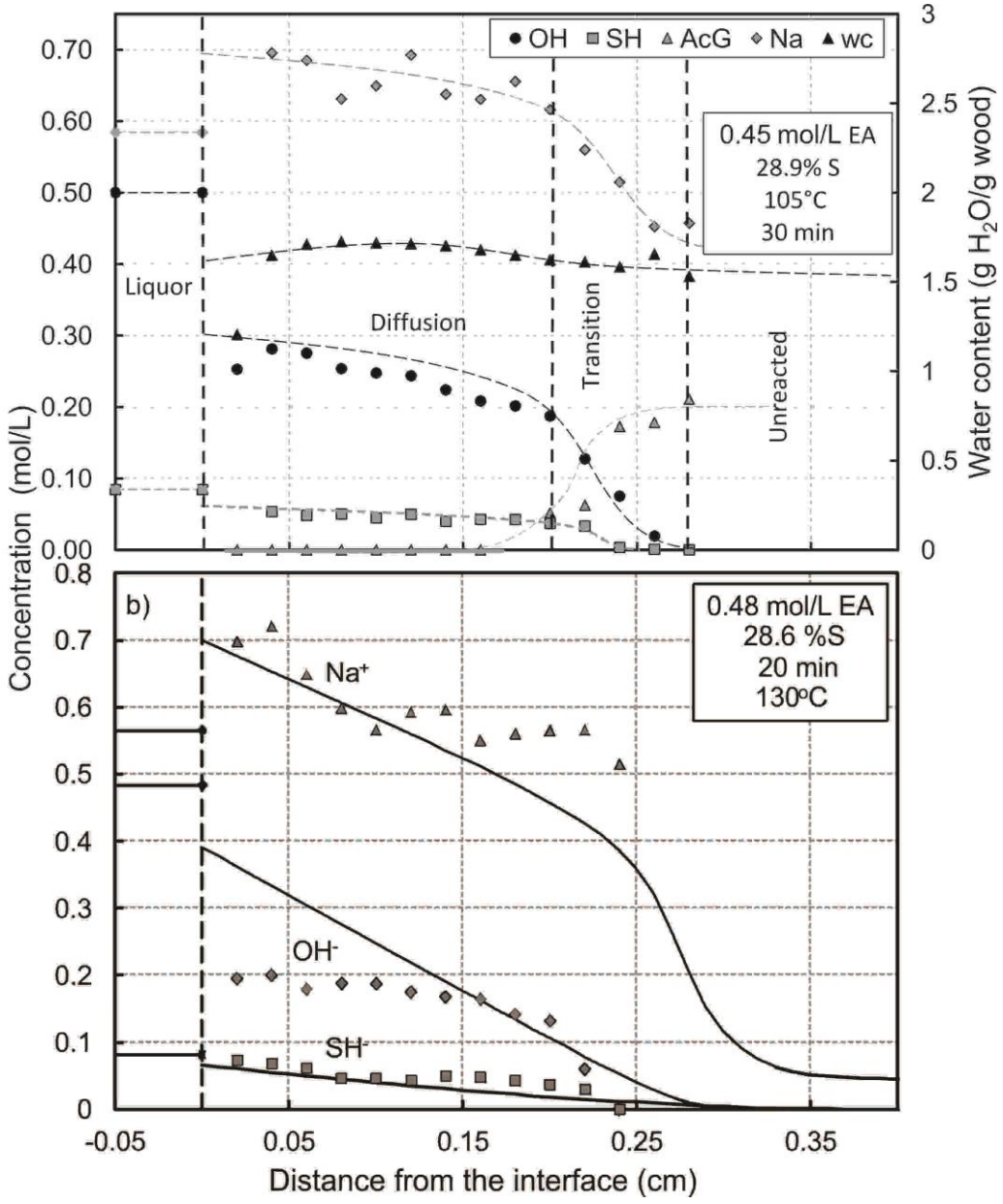

Figure 2. a) Experimental impregnation profiles (EA: 0.45 molNaOH /L, S: 28.9%, 105°C, 30 minutes). **b)** Experimental (point) and simulated (line) impregnation profiles (EA: 0.49molNaOH /L, S: 28.6%, 130°C, 20 min).

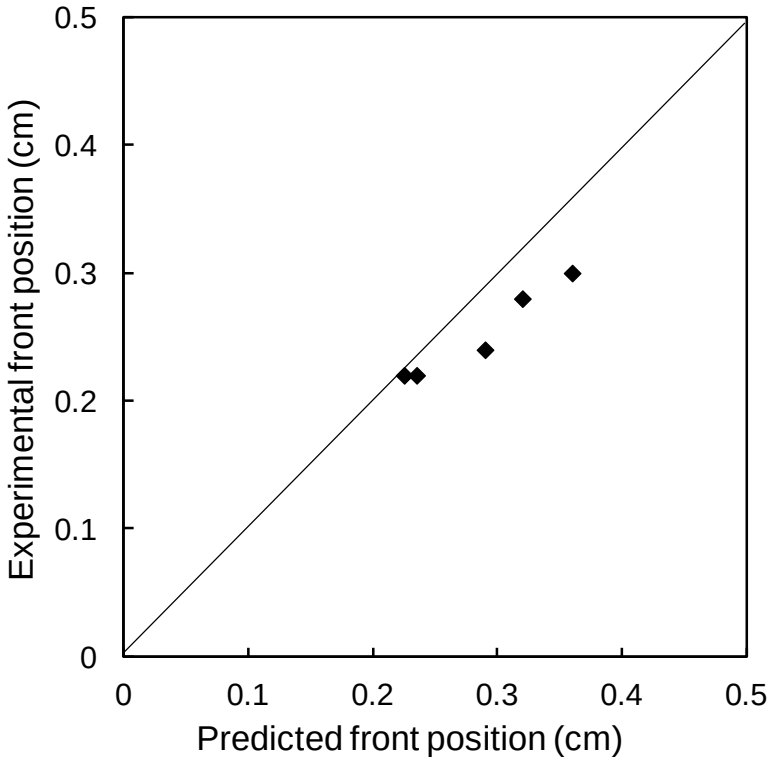

Figure 3. Experimental versus predicted impregnation front positions.

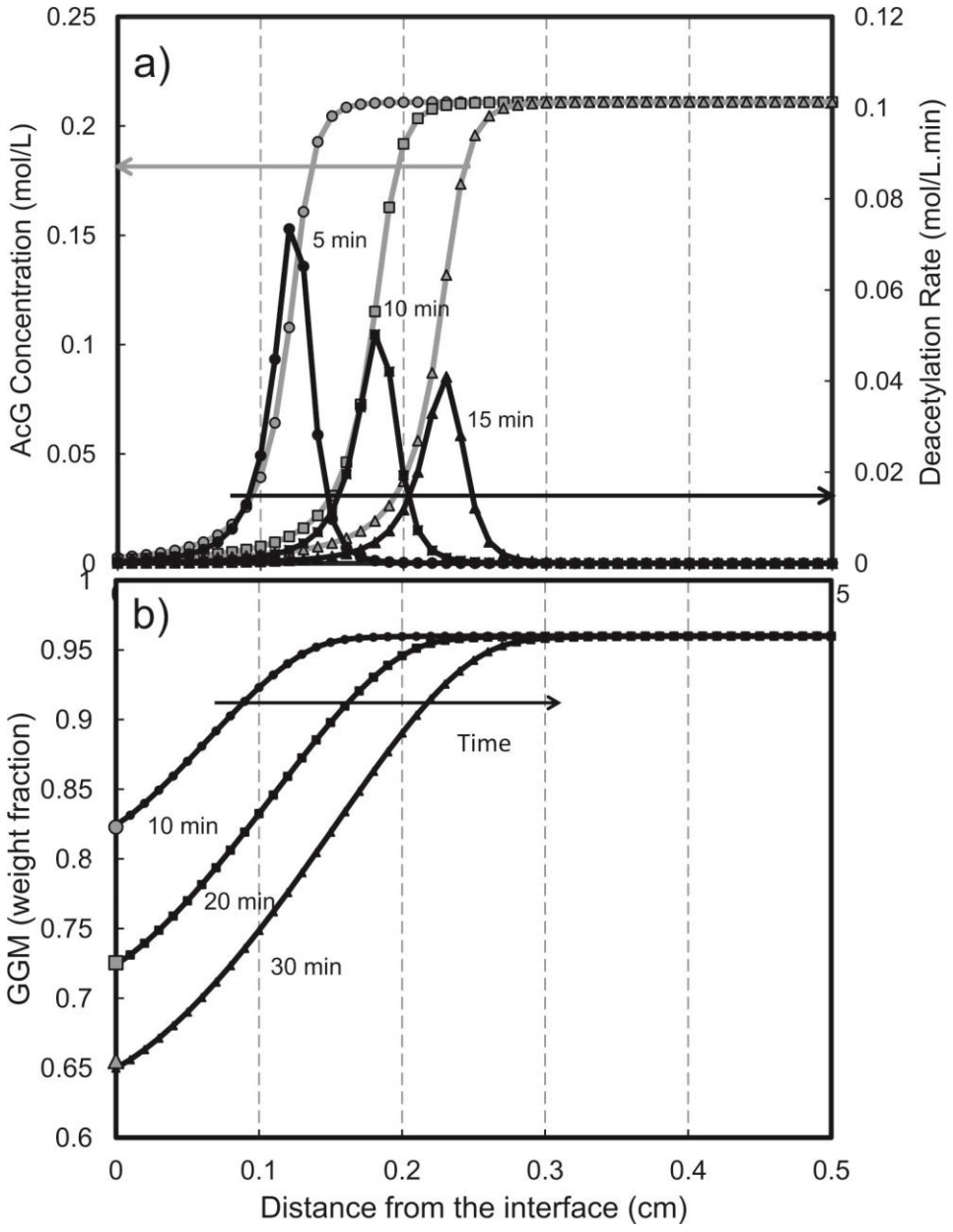

Figure 4. Simulated profiles at different times, **a)** acetyl profiles and the corresponding reaction rate (EA: 0.49molNaOHL^{-1}, S: 28.6%, T: 130°C). **b)** GGM profiles (EA: 0.46 molNaOHL^{-1}, S: 28.9%, T: 105°C). Points indicated in the interphase( ) correspond to GGM calculated using Paananen's kinetic expression.

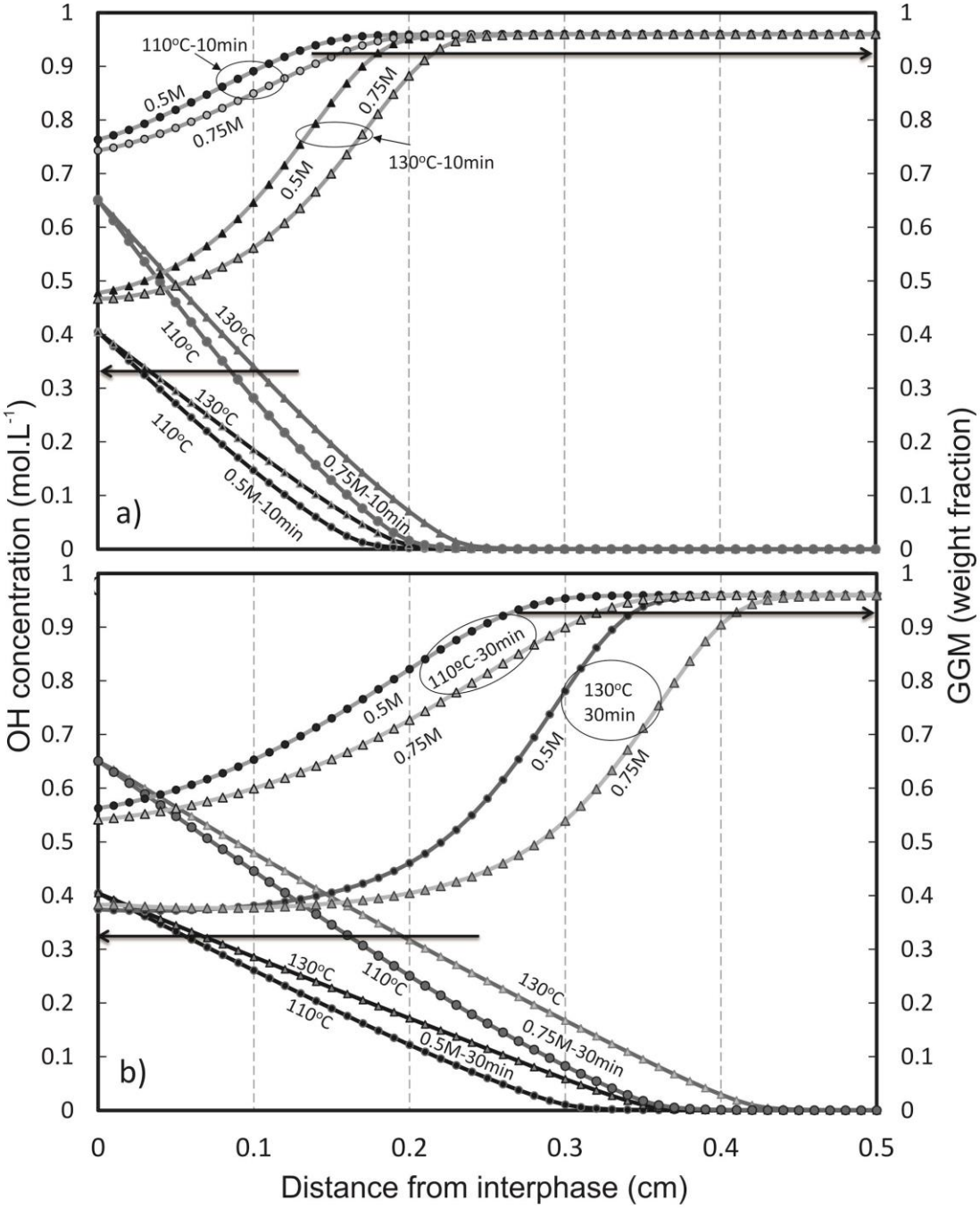

Figure 5. Simulated OH^- and GGM concentration as a function of distances to the interphase at two different temperatures and liquor concentrations.**a)**profiles at 10 min and. **b)** profiles at 30 min.